Vol.4, No.5, Page 2088- 2102, 2026 https://doi.org/10.59628/jast.v4i5.2764 ISSN 2958-9568 JAST

SUN PUBLISHER

مجلة جامعة صنعاء للعلوم التطبيقية والتكنولوجيا

Sana'a University Journal of Applied Sciences and Technology

https://journals.su.edu.ye/index.php/jast/

Green Synthesis, Characterization, and Biological Evaluation of Silver Nanoparticles Using *Rumex nervosus* Flower and Fruit Extracts

Reham Aref [1], Hassan.M. Ibrahim[2], Maher Ali Almaqtari[1] * and Esam M. Aqlan[3]

[1]**Department of Chemistry, Faculty of Sciences, Sana'a University, Sana'a, Yemen,**
[2]**Department of Biology, Faculty Science, Sana'a University, Sana'a, Yemen,**
[3]**Department of Biology, Faculty of Sciences, Ibb University, Ibb, Yemen**

*Corresponding author: m.almaqtari@su.edu.ye

Abstract

Green nanobiotechnology represents a sustainable and cost-effective platform for synthesizing metallic nanoparticles using biologically driven mechanisms. In this study, silver nanoparticles (AgNPs) were biosynthesized for the first time using methanolic and ethanolic extracts of *Rumex nervosus* flowers and fruits. Phytochemical profiling confirmed the presence of phenolics, flavonoids, tannins, and related secondary metabolites in *R. nervosus* flower and fruit extracts, which served as intrinsic reducing and stabilizing agents for AgNP synthesis. The formation of Silver Nanoparticles was indicated by a distinct color transition and further verified by ultraviolet–Visible Spectroscopy, which revealed characteristic surface plasmon resonance. Fourier transform infrared spectroscopy demonstrated notable shifts in the O–H, C=O, C–O, and C–N vibrational bands in the extracts, confirming their involvement in metal ion reduction and capping. X-ray diffraction analysis revealed a face-centered cubic crystalline structure with an average crystallite diameter ranging from 20.7–23.9 nm. Antioxidant evaluation via the 2, 2-diphenyl-1-picrylhydrazyl assay showed that AgNPs exhibited superior radical-scavenging capacity compared to crude extracts, with methanolic AgNPs demonstrating the highest activity (91.69%). Antimicrobial testing revealed that ethanolic AgNPs displayed significant inhibitory activity against gram-negative bacteria, whereas methanolic AgNPs showed negligible effects owing to enhanced nanoparticle stabilization and reduced Ag + availability. These results highlight that *R. nervosus* is an effective biomediator for AgNP formation with promising antioxidant and antibacterial applications.

Article Info

Keywords:
Green synthesis, *Rumex nervosus* Flowers and fruits, Silver Nanoparticles, Characterization, Antioxidant, Antimicrobial

Article History:
Received: 5-February-2026,
Revised: 21-March-2026,
Accepted: 22-March-2026,
Published: 28 May 2026.

1. INTRODUCTION

Bionanotechnology is considered one of the most important branches of nanotechnology because it relies on biological pathways known as green synthesis, which involves the use of plants and microorganisms. This approach is both economical and environmentally friendly because it does not depend on toxic chemicals, high pressure, elevated temperatures, or excessive energy, making it highly applicable in the medical field [1, 2].

Moreover, plants offer several advantages over other biological processes, including risk reduction, cell culture maintenance, and reaction time maintenance [3, 4].

Silver nanoparticles (AgNPs) have gained significant attention in biological applications compared to other metals because of their unique chemical and physical properties [5]. During biosynthesis, plant chemical constituents act as potent reducing agents, facilitating the formation of stable nanoparticles [6].

Recently, the bioactive components of *Rumex nervosus* flowers (Fig.1) were identified, revealing approximately 19 flavonoids for the first time, which act as strong reducing agents in the synthesis of AgNPs [7].

Figure 1. *R. nervosus* flowers and fruits

R. nervosus belongs to the Polygonaceae family, which includes more than 200 species distributed across various countries worldwide.

R. nervosus grows abundantly in several regions of Yemen, where it is a staple in traditional Yemeni medicine. Ethnobotanical records indicate its use in treating inflammatory diseases, diarrhea, wounds, typhoid fever, and various dermatological disorders [8, 9].

Recent pharmacological evaluations have validated these traditional claims, demonstrating that *R. nervosus* extracts possess significant antioxidant, antimicrobial, and anti-inflammatory proper. Notably, the plant exhibits potent urease-inhibitory and anthelmintic activity. Furthermore, studies have identified its potential as an analgesic and antiviral agent against influenza A, exhibiting antileishmanial and cytotoxic (anticancer) activities [10, 11].

Unlike previous studies that focused on leaves [12], this study highlights the unique phytochemical potential of *R. nervosus* flowers and fruits for the rapid synthesis of stable AgNPs.

2. MATERIALS AND METHODS

2.1. Materials

All reagents were of analytical grade and used without further purification. Silver nitrate ($AgNO_3$) was purchased from Fluka-Garantie, and double-distilled water, methanol, and ethanol were purchased from commercial suppliers. Fresh plant samples, flowers, and fruits of *R. nervosus* were collected during the summer of 2024 from Ibb governorate, Yemen. The samples were identified by Dr. Hassan Ibrahim at the Biological Sciences Department, Faculty of Science, Sana'a University, Yemen. More than one sample of each category was assigned herbarium number 1174 and stored at the Faculty of Science Herbarium for reference.

2.2. Methods

2.2.1. Preparation of R. nervosus Flowers and Fruits extracts

Fresh flowers and fruits of *R. nervosus* were collected and washed with tap water, followed by double-distilled water (DD H_2O). The samples were dried at room temperature for 5 days in the absence of sunlight and then pulverized using a sterile electric blender to obtain a fine powder of the same. For extraction, 50 g of powder was separately mixed with 500 mL of methanol (95%) and ethanol (96%). Each mixture was boiled for 35 min at 60℃, cooled, and filtered twice through Whatman No. 1 filter paper. The solvents were then evaporated, and the extracts were concentrated under reduced pressure using a rotary evaporator. The obtained crude extracts were stored at 4℃ until further analysis. [13].

2.2.2. Qualitative Preliminary of Phytochemical Analysis

Following Hoborne [14], a qualitative analysis was conducted to identify a range of bioactive phytoconstituents using freshly prepared methanolic and ethanolic extracts of *R. nervosus* flowers and fruits, to detect alkaloids, glycosides, terpenoids, phenolic compounds, tannins, flavonoids, reducing sugars, and saponins.

2.2.3. Synthesis of AgNPs (Green synthesis)

The green synthesis of *R. nervosus* silver nanoparticles (Rn-AgNPs) was carried out using methanolic and ethanolic extracts of *R. nervosus* flowers and fruits. Each extract was mixed individually with a 0.1 M silver nitrate ($AgNO_3$) solution in a 1:4 ratio. The reaction mixtures were stirred magnetically on a hot plate at 60℃ for 1 h. The formation of Rn-AgNPs was indicated by a visible color change in the solution within 24 h [15, 16].

The nanoparticles were separated via centrifugation at 5000 rpm for 10 min. The resulting precipitate was washed twice with deionized water to remove impurities and then oven-dried to obtain a powder.

2.2.4. Characterization and Measurement Techniques

The green-synthesized silver Rn-AgNPs were characterized using different methods. The optical properties were determined using a UV-Vis double-beam spectrophotometer (Model UV-6100PCS, Shanghai Mapada Instruments Co., Ltd.) at 300–700 nm. Functional group analysis: Fourier transform infrared (FT-IR) spectroscopy (FT/IR-140, Jasco, Japan) was employed, and the ranges of wavenumbers between 4000–400 cm^{-1} were scanned. Finally, to determine the crystalline structure, the crystalline structure of the sample was determined using X-ray diffraction (XRD) at 36 kV and 20 mA, and using Cu Kα ($l = 1.54$ Å) at 36 kV and 20 mA, [17, 18] this analysis was performed by the Geological Survey and

Minerals Resources Board, Yemen.

2.2.5. Zeta Potential Analysis

The zeta potential and colloidal stability of the synthesized AgNPs were evaluated using the method described by Di Fraia *et al.* [19], employing a Zetasizer Nano ZS (Malvern Instruments, UK) equipped with DTS1070 folded capillary cells. The methanol- and ethanol-synthesized AgNPs (individually) were centrifuged, resuspended in deionized water to a concentration of approximately 1 mg/mL, and sonicated for 10 min to ensure homogeneous dispersion. Measurements were conducted at 25℃ with a scattering angle of 173°, and the results were recorded as the average of three independent replicates.

2.2.6. Biological Evaluation of Extracts

2.2.6.1. Antioxidant Activity Evaluation

The antioxidant activity of the *R. nervosus* flowers and fruits methanolic and ethanolic extracts, as well as the nanoparticles derived from each extract, was assessed using a 2, 2-diphenyl-1-picrylhydrazyl (DPPH) free radical scavenging assay [20, 21]. Ascorbic acid was used as the standard.

Antioxidant, and the DPPH solution was prepared by dissolving 2.5 mg DPPH in 25 mL methanol. A 1 mL aliquot of the methanolic DPPH solution was added to different concentrations of ascorbic acid, as well as various concentrations (200, 400, 600, 800, and 1000 $\mu g/mL$) of *R. nervosus* flower and fruit extracts and their corresponding nanoparticles. Each sample was tested individually (all ascorbic acid, plant extracts, and nanoparticles were dissolved in methanol). The control and treated samples (ascorbic acid, plant extracts, and nanoparticle formulations (methanolic and ethanolic Rn-AgNPs) were incubated with the DPPH solution in the dark at room temperature for 30 min. The absorbance was measured at 517 nm using a Genova Life Science Analyzer Protein. The free radical scavenging activity (%) was calculated using the following equation:

$$(\%) = Ac - As/Ac \times 100$$

where is Ac = absorbance of the control sample, and as = absorbance of the test sample (ascorbic acid, plant extracts, or nanoparticles) [20]. In contrast, the half-maximal radical-scavenging activity concentration (IC_{50}) was determined to evaluate the antioxidant potency of the extracts and the synthesized AgNPs. Owing to the significant antioxidant activity observed, where the inhibition percentage exceeded 50% at the lowest tested concentration, the IC_{50} values were calculated using linear interpolation–ratio and proportion– [22, 23]–based on the first data point, according to the following formula:

$$IC_{50} = (50 \times C_1)/RSA1$$

Where C_1 is the lowest concentration tested and RSA1 is the percentage of radical scavenging activity at that concentration. This approach was adopted to provide a more realistic estimation of the IC_{50} within the potent range of the samples and to avoid the statistical bias of the plateau phase observed at higher concentrations.

2.2.6.2.Antimicrobial assays

2.2.6.2.1. Tested Microorganisms:

The antimicrobial activities of *R. nervosus* flower and fruit extracts and the nanoparticle formulations (methanolic and ethanolic Rn-AgNPs) were evaluated against five bacterial strains. These included two gram-positive bacteria, (*Staphylococcus saprophyticus* and *Staphylococcus aureus*), and three gram-negative bacteria (*Escherichia coli*, *Klebsiella pneumoniae*, and *Pseudomonas aeruginosa*). Moreover, the antifungal activity of these extracts and nanoparticle formulations (methanolic and ethanolic Rn -AgNPs) was tested against *Candida albicans*. All microbial isolates were obtained from the National Center of Public Health Laboratories (NCPHL) in Ibb and from Alpha Laboratories.

2.2.6.2.2. Determination of Microbial Activities:

The antimicrobial activities of the methanolic and ethanolic extracts from *R. nervosus* flowers and fruits, as well as their synthesized Rn- AgNPs, were evaluated using the agar well-diffusion method on Mueller Hinton Agar (MHA) for antibacterial testing and Sabouraud dextrose Agar (SDA) for antifungal assessment. The preparation of microbial inocula and the standardization of suspensions were carried out according to the methods described by Ibrahim et al. [20]. To prepare the treatments, a primary stock solution was formulated by dissolving 0.3 g of each extract and AgNPs (individually)in 3 mL of dimethyl sulfoxide (DMSO), yielding an initial concentration of 100 mg/mL. This stock served as the first test concentration and the basis for a twofold serial dilution series. Specifically, the 50 mg/mL concentration was prepared by mixing 1.5 mL of the 100 mg/mL stock with 1.5 mL of pure DMSO. Subsequently, the 25 mg/mL and 12.5 mg/mL dilutions were obtained by sequentially transferring 1.5 mL from the preceding higher concentration into 1.5 mL of fresh DMSO, ensuring a consistent 1:1 dilution ratio at each step. Using a sterile cork borer, wells of 6 mm in diameter were prepared in the agar and filled with 50 μL of each resulting concentration, while 50 μL of pure DMSO was utilized as a negative control [20, 24, 25]. For positive control Ampicillin (AMP) and Chloramphenicol (CHL) served as positive controls for antibacterial activity, while Voriconazole (VRC), Miconazole (MSZ), Fluconazole (FLU), Itraconazole (ITR), Clotrimazole (CLT), and Nystatin (NY) were used as positive controls for antifungal activity. Plates were incubated at 37℃ for 24 h. All procedures were performed in triplicate, and mean inhibition zone diameters (mm) were calculated [24–26].

2.2.6.2.3. Determination of Minimum Inhibitory Concentration (MIC):

The minimum inhibitory concentration (MIC) of the plant extracts and the two AgNP formulations (methanolic and ethanolic) was determined as the lowest level of antimicrobial activity against four test human pathogenic microorganisms (two gram-positive bacteria, *S. saprophyticus* and, *S. aureus*, three gram-negative bacteria, *K. pneumoniae*, *P. aeruginosa*, and *E. coli*) and one fungal pathogen (*C. albicans*)

2.2.6.2.4. Statistical Analysis:

All antimicrobial assays were conducted in triplicate (n=3), and the results are presented as the mean ± standard deviation (SD). To ensure a transparent representation of the experimental data, the variability of the inhibition zones was characterized by reporting the minimum and maximum observed values. [24].

3. RESULTSAND DISCUSSION

3.1. Yield of Plant Extracts

The yield of the crude extracts varied according to the solvent used. Methanol extraction resulted in a higher yield (5.1 g, 10.2% w/w), whereas ethanol extraction yielded 4.20 g (8.4% w/w) relative to the initial 50 g of dry starting material. Based on previous results, methanol extraction resulted in a higher yield than ethanol extraction, which may be attributed to the greater polarity and stronger solvent power of methanol, which enables it to dissolve a wider range or larger quantity of phytochemicals from the plant materials. Studies have shown that **solvents with higher** polarity, such as methanol, tend to extract more phenolic, flavonoid, and hydroxyl-rich compounds, contributing to higher yields and stronger bioactivity [27, 28].

3.2. Phytochemical screening

Phytochemical analysis (Table 1) revealed that the methanolic and ethanolic extracts of *R. nervosus* flowers and fruits contain active compounds, such as alkaloids, phenols, glycosides, and flavonoids. This finding is consistent with previous findings on the 70% methanolic extract of *R. nervosus* flowers [29]. The extracts also contain terpenoids, tannins, reducing sugars, and saponins.

Table 1. The Phytochemical Components of the flowers and fruits methanol and ethanol extracts of *R.nervosus*

Secondary Metabolites	Test Reagent	Method of Extraction	
		Methanol	Ethanol
Alkaloids	Wanger ’s test	+	+
Flavonoids	Ferric Chloride	+	+
	Lead acetate	+	+
Terpenoids	Salkowski	+	+
Phenol	Ferric Chloride	+	+
Tannins	Ferric Chloride	+	+
Glycosides	Keller-Killani	+	+
Reducing Sugar	Fehling ’s test	+	+
Saponins	Foam test	+	+
“+ “: the active compound is presented			

3.3. Ultraviolet-Visible (UV-Vis) analysis:

A distinct color change from pale to dark was observed in the methanolic and ethanolic extracts of *R. nervosus* flowers and fruits after adding $AgNO_3$, indicating the successful formation of Rn-AgNPs within one hour due to surface Plasmon Resonance (SPR). As shown in Fig. 2, the UV-Visible absorption spectrum displayed SPR peaks at approximately 380–324 nm and 345–324 nm, confirming the reduction of Ag^+ ions and the synthesis of AgNPs, respectively. This wavelength range reflects the small size, stability, and minimal aggregation of the nanoparticles, as smaller particles cause collective electron oscillations at higher energies, resulting in a blue shift to shorter wavelengths. [30, 31].

3.4. Fourier Transform Infrared (FT-IR) Spectroscopy Analysis

Table 2 and Figs.3 and 4 present the FTIR spectra of *R. nervosus* flower and fruit ethanolic and methanolic extracts, along with their corresponding Rn-AgNPs. The observed spectral variations confirm the involvement of plant phytochemicals in nanoparticle formation. A shift in the O–H stretching vibration was observed following nanoparticle synthesis. In the ethanolic extract, the O–H band decreased from 3497.76 cm^{-1} (Fig.3 A) to 3431.71 cm^{-1} (Fig.4 A) in the ethanol Rn-AgNPs, while in the methanolic extract, it shifted from 3422.06 cm^{-1} (Fig.3 B) to 3396.03 cm^{-1} in methanol Rn-AgNPs (Fig.4 B). This downward shift indicates that hydroxyl-containing compounds, mainly phenolics and flavonoids, participated in reducing Ag^+ to Ag^o and were partially consumed in the process. These compounds also adsorbed onto the nanoparticle surface, contributing to capping and stabilization. The carbonyl (C=O) stretching bands also shifted, from 1718.26 in ethanol extract (Fig.3 A) to 1707.66 cm^{-1} in ethanol Rn-AgNPs (Fig.4 A) and from 1708.62 in methanol (Fig.3 B) extract to 1700.91 cm^{-1} in methanol Rn-AgNPs (Fig.4 B). These changes confirm the role of carbonyl groups as electron donors and stabilizing agents during nanoparticle formation. Additional spectral changes were noted in the C–N and C–O functional groups. The C–N band shifted from 1384.64 and 1383.68 cm^{-1} in the ethanol and methanol crude extracts, respectively (Fig.3 A & B) to 1364.39 and 1365.35 cm^{-1} in Rn- AgNPs ethanol and methanol, respectively (Fig.4 A & B). The C–O stretching bands shifted from 1033.66 and 1208.18 cm^{-1} in the ethanol and methanol crude extracts,

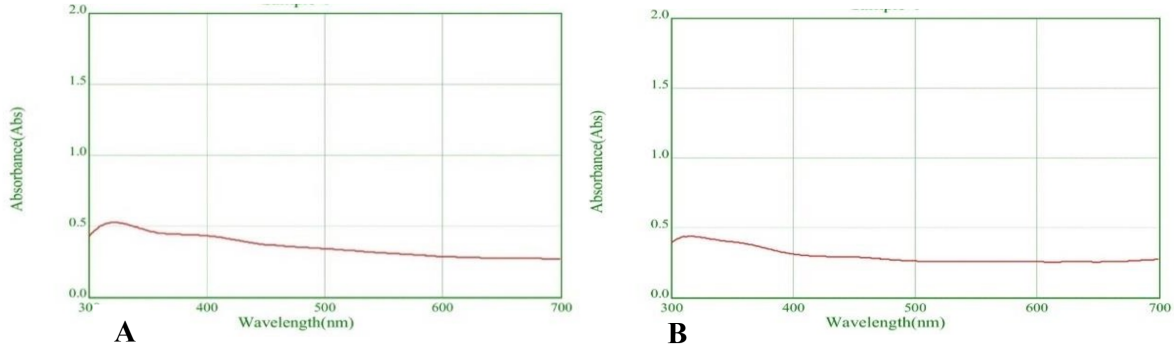

Figure 2. UV-Vis absorption spectrum of Rn-AgNPs prepared using *R. nervosus* flowers and fruits (**A**) Methanol, (**B**) Ethanol extracts

Table 2. FT-IR Spectrum of *R.nervosus* flower and fruit extracts and silver nanoparticles (Rn- AgNPs)

NO	Functional group	Wave number of absorption cm^{-1}			
		Ethanol		Methanol	
		Extract	Rn-AgNPs	Extract	Rn-AgNPs
1	-OH	3497.76	3431.71	3422.06	3396.03
2	-CH (Alkanes/Aliphatic)	2923.56	2922.59	2921.63	2854.13
3	-C=O	1718.26	1707.66	1708.62	1700.91
4	-C=C	1618.95	1617.02	1617.98	1609.31
5	C-N	1384.64	1364.39	1383.68	1365.35
6	C-O-	1033.66	1035.59	1208.18	1052.94
7	-C-H (out of plan - OOP)	873.596	520.686	670.142	521.65

correspondingly (Fig.3 A & B) to 1035.59 and 1052.94 cm^{-1} in Rn-AgNPs ethanol and methanol, respectively (Fig.4 A & B). These shifts reflect an interaction between the extracted biomolecules, and the nanoparticle surface. A pronounced decrease in the aromatic C–H out-of-plane vibration was also detected, shifting from 873.59 and 670.14 cm^{-1} in the extracts (Fig.3 A & B) to approximately 520 cm^{-1} in the synthesized nanoparticles (Fig.4 A & B). This reduction provides additional confirmation of successful Rn- AgNP capping and surface modification. Overall, these FT-IR spectral changes show that phenolic, carbonyl, and amine-containing phytochemicals act as reducing agents, converting Ag^{+} to Ag^{0}. In addition, proteins and polysaccharide-like compounds contribute to nanoparticle capping and stabilization [32].

3.5. X-ray Diffraction analysis

Fig. 5 A&B present the X-ray diffraction (XRD) patterns of AgNPs prepared using *R. nervosus* flower and fruit methanolic and ethanolic extracts individually. These patterns confirm the phase purity of the crystalline structures. For the methanolic extract, three sharp peaks appear at 2θ values of 38.755°, 44.101°, and 64.540°. However, for the ethanolic extract, the peaks are at 38.000°, 44.221 °, and 64.580°. These peaks correspond to the 111, 200, and 220 crystallographic planes (Table 3). The sharp and intense peaks indicate that the synthesized Rn-AgNPs are highly crystalline. The average crystallite sizes (D) were 23.931 and 20.713 nm, prepared using *R. nervosus* flower and fruit methanolic and ethanolic extracts, respectively (Table 3). These values were calculated using the Scherrer equation.

$$D = 0.9\lambda / \beta \cos\theta$$

where λ = 0.154 nm, θ is the diffraction angle, and β is the full width at half maximum, which was used to calculate the crystallite size [33]. XRD analysis of the AgNPs synthesized using *R. nervosus* flower and fruit confirmed the formation of highly crystalline, phase-pure metallic silver. The diffraction patterns of both extracts exhibited three distinct sharp peaks corresponding to the (111), (200), and (220) crystallographic planes. Specifically, the methanolic extract showed peaks at 2θ values of 38.755°, 44.101°, and 64.540°, whereas the ethanolic extract showed peaks at 38.000°, 44.221°, and 64.580°. These values are in excellent agreement with the standard face-centered cubic (FCC) structure of silver reported in the literature. The sharpness and high intensity of these peaks further indicate the high degree of crystallinity of the biosynthesized nanoparticles. Based on Scherrer's equation, the average crystallite sizes were determined to be 23.931 nm and 20.713 nm

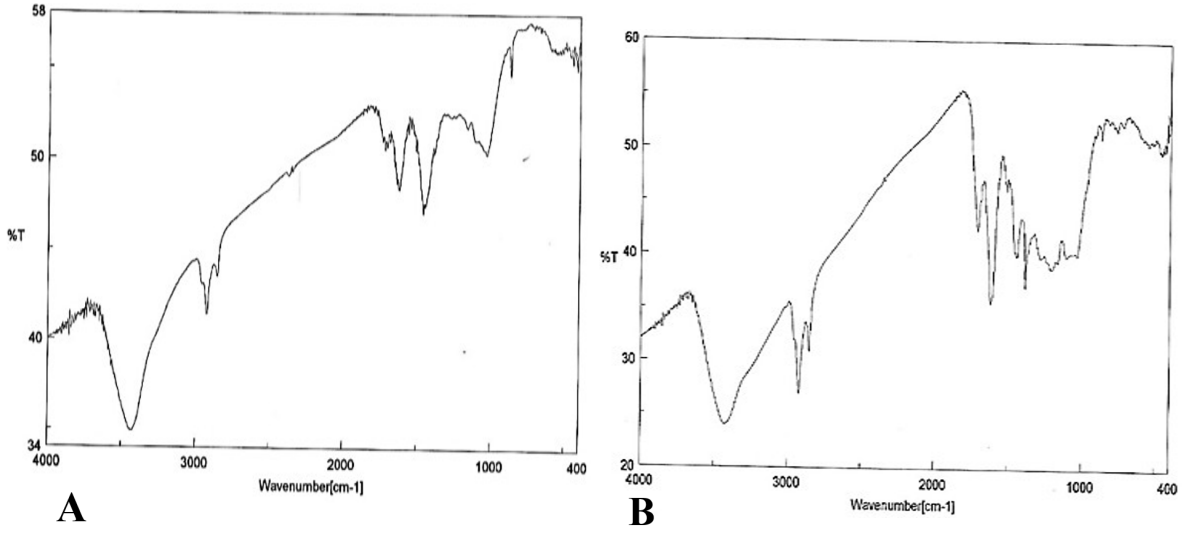

Figure 3. FT-IR Spectrum analysis of the Ethanol (A), Methanol (B) extracts of *R. nervosus* flowers

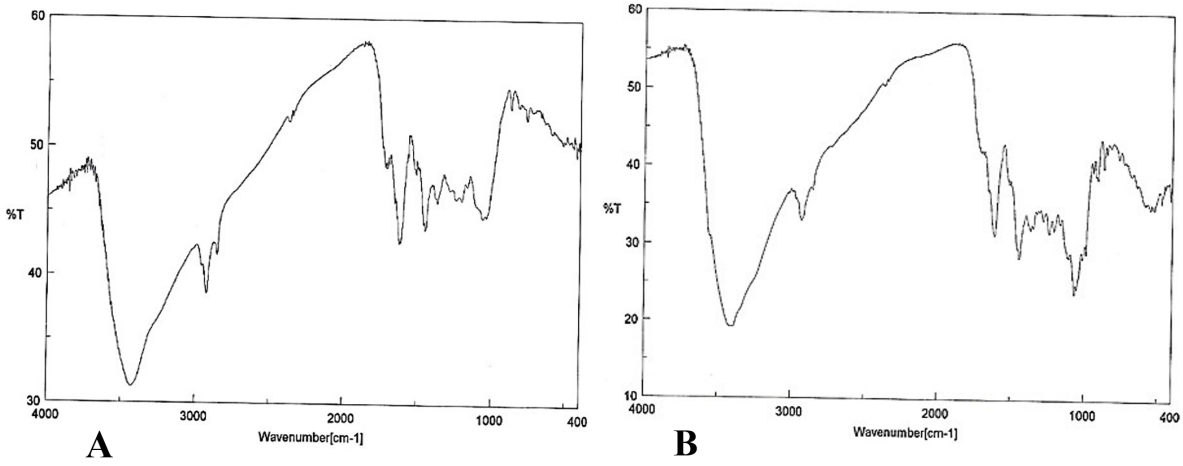

Figure 4. FT-IR Spectrum analysis of Rn-AgNPs prepared using Ethanol (A), Methanol (B) extracts of *R. nervosus* flowers and fruits

for the methanolic and ethanolic extracts, respectively. These dimensions are consistent with previous green synthesis studies [18], which typically yield nanoparticles in the 10–50 nm range, proving that *R. nervosus* phytochemicals act as efficient reducing and stabilizing agents.

The crystalline nature and mean size of the synthesized AgNPs were confirmed by XRD analysis using the Scherrer equation. This approach provides a statistically valid estimation of the crystallite size, which is in good agreement with the SPR peaks observed in the UV-Vis spectra.

3.6. Zeta Potential Analysis

The zeta potential is a fundamental parameter used to quantify the surface charge of nanoparticles, which directly influences the physical stability and aggregation behavior of colloidal dispersions. The AgNPs synthesized using *R. nervosus* methanolic and ethanolic extracts exhibited significant negative zeta potential values (-25.6 ±0.1 and -28.4 ± 02 mV. respectively). These negative values suggest that the nanoparticles were effectively capped by anionic phytochemicals, such as phenolics, flavonoids, and organic acids, present in the plant extracts. Furthermore, this surface charge creates substantial electrostatic repulsion that maintains particle dispersion and reduces aggregation, indicating that AgNPs possess moderate to high colloidal stability [34, 35].

3.7. DPPH Scavenging Activity of Determination of the flowers and fruits extracts and AgNPs of *R. nervosus*.

Determination of DPPH scavenging activity of the flower and fruit extracts and Rn-AgNPs of *R. nervosus*. This method is based on the reduction of the stable purple DPPH free radical in the presence of an antioxidant agent, resulting in its conversion to the yellow non-radical

Table 3. X-ray diffraction (XRD) characteristics of the synthesized and standard AgNPs.

R.nervosus flower and fruit extracts	Metal	2-theta (2 θ)	(hkl)	FWHM (β)	Crystallite size(D,nm)	Average (D,nm)
Methanol	Ag	38.75	111	0.4	21.986	23.931
		44.101	200	0.388	23.07	
		64.54	220	0.367	26.74	
Ethanol	Ag	38.0	111	0.544	16.1296	20.713
		44.221	200	0.381	23.5	
		64.58	220	0.436	22.5096	

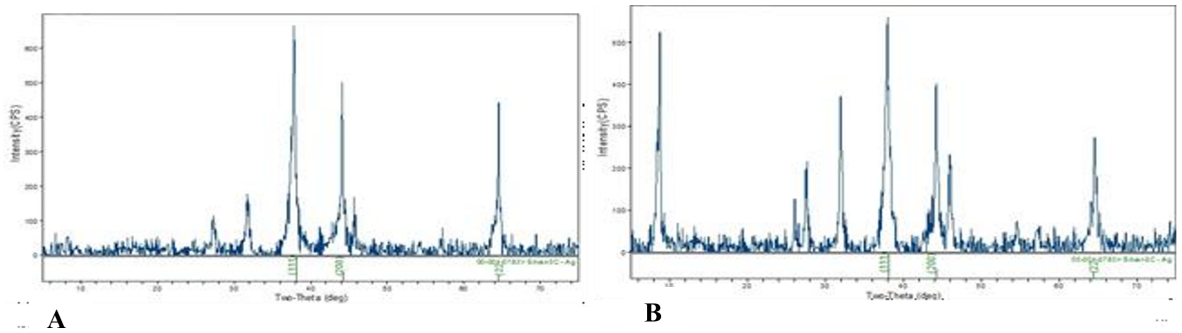

Figure 5. X-ray diffraction (XRD) pattern of AgNPs synthesis using Methanol (A), Ethanol (B) *R. nervosus*

form. Table 4 and Fig. 6 summarize the free radical scavenging activity of the *R. nervosus* flower fruit methanolic and ethanolic extracts and the AgNPs synthesized using each extract individually. The radical-scavenging activity (RSA%) of *R. nervosus* flower and fruit extracts and their silver nanoparticle formulations (Rn-AgNPs) increased proportionally with increasing concentrations (Fig. 6). Ascorbic acid exhibited the highest efficiency at low concentrations, reaching 90.9% at 10 $\mu g/mL$ concentration. Among the plant-derived samples, the methanolic nanoparticle formulation (Rn-AgNPs) showed the highest antioxidant response (91.697% at 1000 $\mu g/mL$), outperforming the pure methanolic (78.73%) and ethanolic (86.089%) extracts. Additionally, the ethanolic nanoparticle formulation (Rn-AgNPs) demonstrated improved radical-scavenging activity (87.036%) compared to its crude extract. The methanolic nanoparticle formulation (Rn-AgNPs) exhibited improved radical-scavenging activity (91.697%) compared to the crude extract. Overall, the conjugation of the plant was determined to be 23.931 nm for the methanolic extract and 20.713 nm for the ethanolic extract. These dimensions are consistent with previous green synthesis studies, which typically yield nanoparticles in the 10–50 nm range, proving that *R. nervosus* phytochemicals act as efficient reducing and stabilizing agent extracts with AgNPs markedly enhanced their antioxidant capacity. The methanolic nanoparticle formulation showed the strongest effect due to its higher polarity, which enables broader extraction of phenolic compounds and flavonoids, the primary contributors to antioxidant activity and reducing factors required for the formation of AgNPs [10, 36]. Several studies have confirmed that biologically synthesized nanoparticles display stronger antioxidant activity than their corresponding plant extracts [37].

According to the formula $IC_{50} = (50 \times C_1)/RSA1$ and table x, the lowest concentration that gives the half-maximal radical scavenging activity percentage IC_{50} was 118.6 $\mu g/ml$ for the Methanol Rn-AgNPs, followed by Ethanol Rn-AgNPs and Ethanol extract with concentrations of 120.2 and 132.2 $\mu g/ml$, respectively, while the highest concentration that gives half-maximal the radical scavenging activity percentage (IC_{50}) was for Methanol extract with a concentration of 138.1 $\mu g/ml$, this agrees with many studies where they reported that the AgNPs synthesized using methanol exhibited higher antioxidant potency, as reflected by lower IC_{50} values, than ethanolic AgNPs across various plant sources [38–40].

3.7.1. Determination of Antimicrobial Activity

Table 5 and Fig.7. illustrates that the *R. nervosus* flowers and fruits methanolic extract showed an antibacterial against one positive gram bacteria; *S. aureus* at high concentration (100 mg/ml) with a mean inhibition zone 13.3 mm, however it did not demonstrate any activates against S. saprophyticus. Furthermore, the *R. nervosus* flowers and fruits ethanolic extract at four concentrations (100, 50, 25, and 12.5 mg/ml) exhibited antibacterial activity against *S. aureus* with a mean inhibition zone of 18.3, 14, 11.7, and 11 mm, respectively, but did not show any activity against *S. saprophyticus* (Table 5) and Fig.8. Moreover, the methanolic and ethanolic Rn-AgNP extracts did not exhibit any activity against the selected gram-positive bacteria (Table 5). Conversely, the *R. ner-*

Table 4. The antioxidant activity of *R. nervosus* flower and fruit extracts and silver nanoparticles (Rn-AgNPs)

Radical Scavenging of *R.nervosus* flowers and fruits extracts and silver nanoparticles (Rn-AgNPs)													
N O	Concentration ($\mu g/ml$)	Methanol						Ethanol					
		Extract			AgNPs			Extract			AgNPs		
		Ab	RSA%	IC_{50} $\mu g/ml$	Ab	RSA%	IC_{50} $\mu g/ml$	Ab	RSA%	IC_{50} $\mu g/ml$	Ab	RSA%	IC_{50} $\mu g/ml$
1	200	0.370	73.052		0.213	84.487		0.334	75.674		0.226	83.54	
2	400	0.334	75.674		0.143	89.585		0.317	76.912		0.204	85.142	
3	600	0.314	77.130	138.1	0.140	89.803	118.6	0.239	82.593	132.2	0.188	86.307	120.2
4	800	0.303	77.932		0.136	90.095		0.210	84.705		0.185	86.526	
5	1000	0,292	78.73		0.114	91.697		0.191	86.089		0.178	87.036	
Ab Absorbance, RSA% Radical scavenging activity percentage													

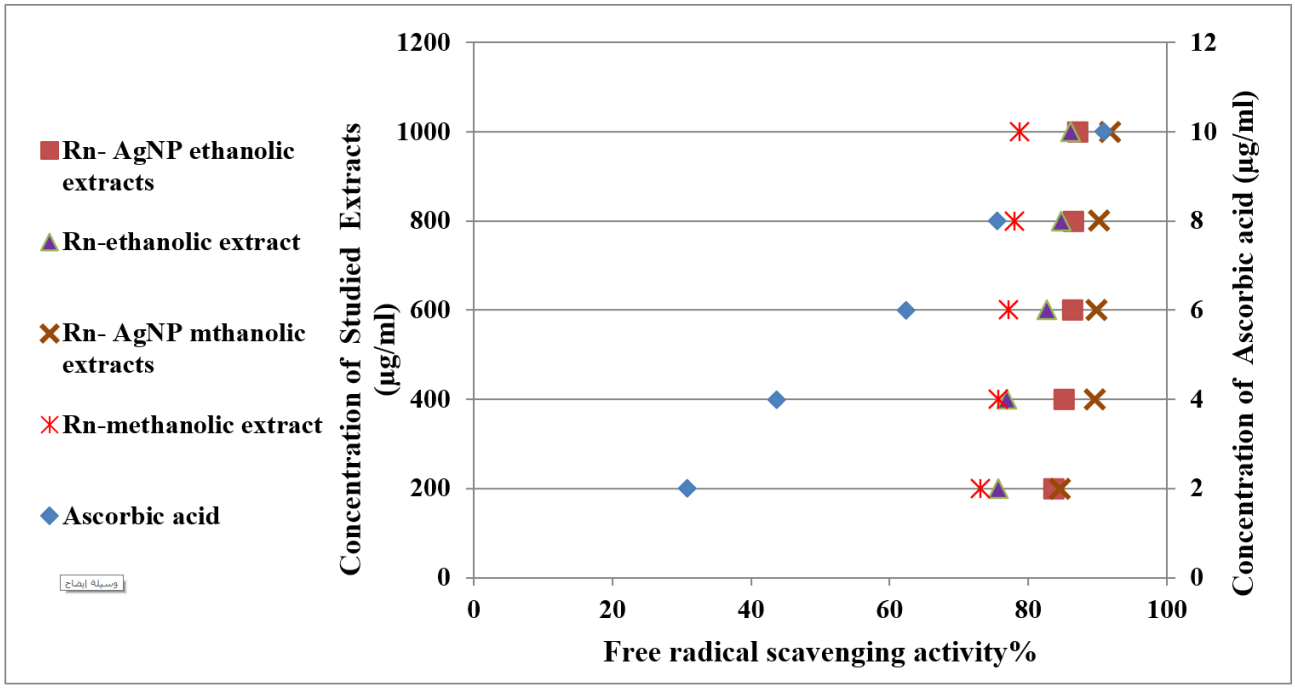

Figure 6. Free radical scavenging activity% of *R. nervosus* flowers and fruits extracts and silver nanoparticles (Rn-AgNPs)

vosus flowers and fruits methanolic extract demonstrated antibacterial activity against the selected gram-negative bacteria, producing a mean inhibition zone of 10.3, 10, 7, and 5.3 mm against *E. coli* and 17.3, 15.7, 15.3, and 13 against *P. aeruginosa* at concentrations of 100, 50, 25, and 12.5 mg/ml, respectively. It also produced a mean inhibition zone of 12.7 mm against *K. pneumoniae* at a concentration of 100 mg/ml (Table 5) and Fig.7. However, the *R. nervosus* flowers and fruits ethanolic extract exhibited antibacterial activity against two gram-negative bacteria, *E. coli*, with a mean inhibition zone of 10.7, 10.3, 7.7, and 6.7 at concentrations of 100, 50, 25, and 12,5 mg/ml, respectively, and *K. pneumoniae*, with an inhibition zone of 13.3, 11.7, 11.3, and 10.3 at concentrations of 100, 50, 25, and 12,5 mg/ml sequentially. However, it did not demonstrate any activity against *P. aeruginosa* (Table 5) and Fig.8. Additionally, methanol Rn-AgNP displayed antibacterial activity against two gram-negative bacteria (*E. coli* and *P. aeruginosa*). For *E. coli* it produces a mean inhibition zone of 10.3, 9.7, 9.3 and 9 mm at concentrations of 100, 50, 25 and 12,5 mg/ml correspondingly, while against *P. aeruginosa* the mean inhibition zones were 15.7, 14.7, 13.7 and 10.3 mm at concentrations of 100, 50, 25, and 12.5 mg/mL, respectively; however, it showed no activity against *K. pneumoniae* (Table 5) and Fig.7. In contrast, ethanolic Rn-AgNP exhibited antibacterial activity against all three selected gram-negative bacteria, with a mean inhibition zone of 15, 11, 9.7, and 9.3 mm against *E. coli* at concentrations of 100, 50, 25, and 12.5 mg/ml, respectively, whereas it displayed antimicrobial activity with a mean inhibition zone of 10, 9.3, and 8.7 mm against *K. pneumoniae* and 12.7, 11.7, and 10.3 mm against *P. aeruginosa* at concentrations of 100, 50, and 25 mg/ml, respectively (Table 5) and Fig.8 In addition to antibacterial activity, the extracts also demonstrated antifungal activity against *C. albicans* (Table 5) with mean inhibition zones of 10.7, 9.7, 9, and 8.7 mm at concentrations of 100, 50, 25, and 12.5 mg/mL, respectively, for the *R. nervosus* flowers and fruits methanolic extract, while the ethanolic *R. nervosus* flowers and fruits extract exhibited antifungal activity with mean inhibition zones of 13, 11.7, and 10 mm at concentrations of 100, 50, and 25

mg/mL, respectively. Furthermore, methanol Rn-AgNP did not show any antifungal activity against *C. albicans*, whereas ethanolic Rn-AgNP displayed antifungal activity against *C. albicans* at a concentration of 100 mg/mL with a mean inhibition zone of 10.7 mm (Table 5) and Fig.7,8. According to Table 5, Fig.9 the antibiotics Ampicillin and Chloramphenicol antibiotics demonstrated antibacterial activity against *S. aureus*, with inhibition zones of 19 and 24 mm, respectively. Moreover, Chloramphenicol also exhibited an antibacterial activity against S. saprophyticus, with an inhibition zone of 20 mm, while Ampicillin did not show any activity against S. saprophyticus. Furthermore, the three selected gram -negative bacteria exhibited a resistant to Ampicillin antibiotic, whereas Chloramphenicol showed an antibacterial activity against the three selected gram-negative bacteria; *E. coli*, *K. pneumoniae* and *P. aeruginosa* with inhibition zone of 30, 10 and 18 correspondingly (Table 5 and Fig.9).

In contrast, the antibiotics Nystatin, Clotrimazole, Fluconazole, Miconazole and Voriconazole displayed antifungal activity against *C. albicans*, with inhibition zones of 22, 12, 30, 11, and 31 mm, respectively, while the antibiotic itraconazole did not exhibit any antifungal activity against *C. albicans* (Table 5 and Fig.10). Table 6 demonstrates that Rn-AgNP in methanol exhibited no antimicrobial activity, unlike the ethanolic Rn-AgNP. This may be attributed to the higher concentrations of polar phytochemicals, such as polyphenols, flavonoids, tannins, and saponins, in the methanolic extracts compared to the ethanolic extracts. These phytochemicals act as reducing and capping agents during nanoparticle synthesis, enhancing the stability of nanoparticles, including AgNPs, and consequently reducing or halting the antimicrobial activity of AgNPs in methanol Rn-AgNPs [41–43].

3.7.2. Minimum Inhibitory Concentration (MIC)

Based on Table 5, the Minimum Inhibitory Concentration (MIC)of the methanolic *R. nervosus* flower and fruit extracts was 100,12.5,100,12.5and 12.5 mg/ml against *S. aureus*, *E. coli*, *K. pneumoniae, P. aeruginosa*,and *C. albicans*,with mean inhibition zones of 13.3, 5.3,12.7,and 8.7 mm, respectively.H owever, the *R. nervosus* flower and fruit extracts showed MIC values of 12.5, 12.5,12.5and 25 mg/ml with mean inhibition zones of 11, 6.7, 10.3, and 10.7 mm against *S. aureus, E. coli, K. pneumoniae* and *C. albicans* respectively (Table 5). Furthermore, the MIC of methanolic Rn-AgNPs was 12.5 mg/ml against *E. coli* and *P. aeruginosa* with mean inhibition zones of 9 and 10.3 mm, respectively (Table 5) . In addition, the ethanolic Rn-AgNPs displayed MIC of 12.5, 25, and 25 mg/ml with mean inhibition zones of 9.3, 8.7, and 10.3 against *E. coli*, *K. pneumoniae*, and *P. aeruginosa*, respectively (Table 5).

As shown in Table 5, the *ethanolic extract of R. nervosus flowers and fruits* exhibited greater antibacterial activity against *S. aureus* (gram-positive bacteria) and *K. pneumoniae* (gram-negative bacteria) than the methanolic extract of *R. nervosus* flowers and fruit. This maybe attributed to the difference in polarity between ethanol and methanol, where methanol is slightly more polar, and this difference influences their ability to dissolve various phytochemicals. Therefore, Ethanol can extract a broader spectrum of bioactive compounds (both polar and moderately non-polar compounds), which can be more efficient as an antimicrobial agent [41–43]. In addition, ethanol frequently yields metabolite profiles with synergistic antimicrobial potential, as it extracts diverse classes of bioactive compounds, including phenolics, flavonoids, terpenoids, and fatty acids, which can act synergistically to enhance antibacterial activity [44–46]. Moreover, the results in Table 5 illustrate that neither the methanolic nor ethanolic extracts of *R. nervosus* flowers and fruits, nor their corresponding Rn-AgNPs, exhibited antibacterial activity against *S. saprophyticus*. This absence of inhibition may be attributed to resistance mechanisms inherent to the clinical strain, such as active efflux systems, biofilm formation, or structural modifications of the cell envelope, which limit the penetration or effectiveness of the plant-derived antimicrobial compounds. Such traits are common in isolates obtained from medical laboratories, where selective pressure often causes resistance to both synthetic and natural antimicrobials [47, 48]. In addition, Table 5 indicates that *P. aeruginosa* was resistant to the ethanolic extract but sensitive to the methanol extract. This may be because *P. aeruginosa* has a robust outer membrane, efflux pumps, and biofilm-forming capacity, and only compounds with certain physicochemical properties can penetrate or disrupt them [49]. However, methanolic extracts may contain compounds capable of permeabilizing or inhibiting these defenses, whereas ethanolic extracts may lack these compounds [50, 51].

Moreover, the results in Table 5 demonstrate that methanol Rn-AgNPs exhibited no antimicrobial activity, unlike the ethanolic Rn-AgNPs. This may be attributed to the higher concentrations of polar phytochemicals, such as polyphenols, flavonoids, tannins, and saponins, in the methanolic extracts than in the ethanolic extracts. These phytochemicals act as reducing and capping agents during nanoparticle synthesis, enhancing the stability of nanoparticles, including AgNPs, and consequently reducing or halting the antimicrobial activity of AgNPs in methanol Rn-AgNPs [52–54].

4. CONCLUSION

This study successfully established the flowers and fruits of *R. nervosus* as a novel biogenic platform for the synthesis of crystalline nanoscale silver particles. The novelty of this study lies in the specific utilization of these reproductive plant organs. While previous research has

Table 5. Inhibition zone diameters (mm) of methanolic and ethanolic extracts and silver nanoparticles (Rn- AgNPs) against tested Pathogens

Test Sample	Concentration(mg/ml)	Inhibition zone diameter (mm)											
		Test microorganisms											
		Gram-positive bacteria				Gram-negative bacteria						Fungus	
		S. aureus		*S. saprophyticus*		*E. coli*		*K. pneumoniae*		*P. aeruginosa*		*C. albicans*	
		Extract Min (Mean ±SD) Max	Rn-AgNPs Min (Mean ±SD) Max	Extract Min (Mean ±SD) Max	Rn-AgNPs Min (Mean ±SD) Max	Extract Min (Mean ±SD) Max	Rn-AgNPs Min (Mean ±SD) Max	Extract Min (Mean ±SD) Max	Rn-AgNPs Min (Mean ±SD) Max	Extract Min (Mean ±SD) Max	Rn-AgNPs Min (Mean ±SD) Max	Extract Min (Mean ±SD) Max	Rn-AgNPs Min (Mean ±SD) Max
Methanol	100	13 (13.3 ±0.6) 14	-	-	-	10 (10.3±0.6) 11	10 (10.3±0.6) 11	12 (12.7±0.58) 13	-	17 (17.3±0.6) 18	15 (15.7±0.6) 16	10 (10.7±0.6) 11	-
	50	-	-	-	-	10	9 (9.7±0.6 10	-	-	15 (15.7±0.6) 13	14 (14.7±0.6) 15	9 (9.7±0.6) 10	-
	25	-	-	-	-	6 (7±1) 8	9 (9.3±0.6) 10	-	-	15 (15.3±0.6) 16	13 (13.7.3±0.6) 14	8 (9±1) 10	-
	12.5	-	-	-	-	5 (5.3±0.6) 6	8 (9±1) 10	-	-	12 (13±1) 14	10 (10.3±0.6) 11	8 (8.7±0.6) 9	-
	6.25	-	-	-	-	-	-	-	-	-	-	-	-
Ethanol	100	18 (18.3 ±0.6) 19	-	-	-	10 (10.7±1.2) 12	14 (15±1) 16	13 (13.3±0.6) 14	9 (10±1) 11	-	12 (12.7±0.6) 13	12 (13±1) 14	10 (10.7-±0.6) 11
	50	13 (14 ±1) 15	-	-	-	10 (10.3±0.6) 11	10 (11±1) 12	11 (11.7±0.6) 12	9 (9.3±0.6) 10	-	11 (11.7±0.6) 12	11 (11.7±0.6) 12	-
	25	11 (11.7 ±0.6) 12	-	-	-	7 (7. 7±0.6) 8	9 (9.7±0.6) 10	11 (11.3±0.6) 12	8 (8.7±0.6) 9	-	10 (10.3±0.6) 11	10 (10.7-±0.6) 11	-
	12.5	11	-	-	-	6 (6.7±0.6) 7	9 (9.3±0.6) 10	9 (10.3±1.5) 12	-	-	-	-	-
	6.25	-	-	-	-	-	-	-	-	-	-	-	-
Negative control (DMSO)-		-		-		-		-		-			
Positive control (Bacterial Antibi-otics)	AMP (25)	19	-	-		-		-		-		Positive control (Fungal Antibiotics)	NY (100) 22
													ITR (50) -
	CHL (30)	24	-	20		30		10		18			CLT(50) 12
													FLU (25) 30
													MSZ (10) 11
													VRC (1) 31

"- ": no activity, AMP: Ampicillin, CHL: Chloramphenicol, NY: Nystatin, ITR: Itraconazole, CLT: Clotrimazole, FLU: Fluconazole, MSZ: Miconazole and VRC Voriconazole.

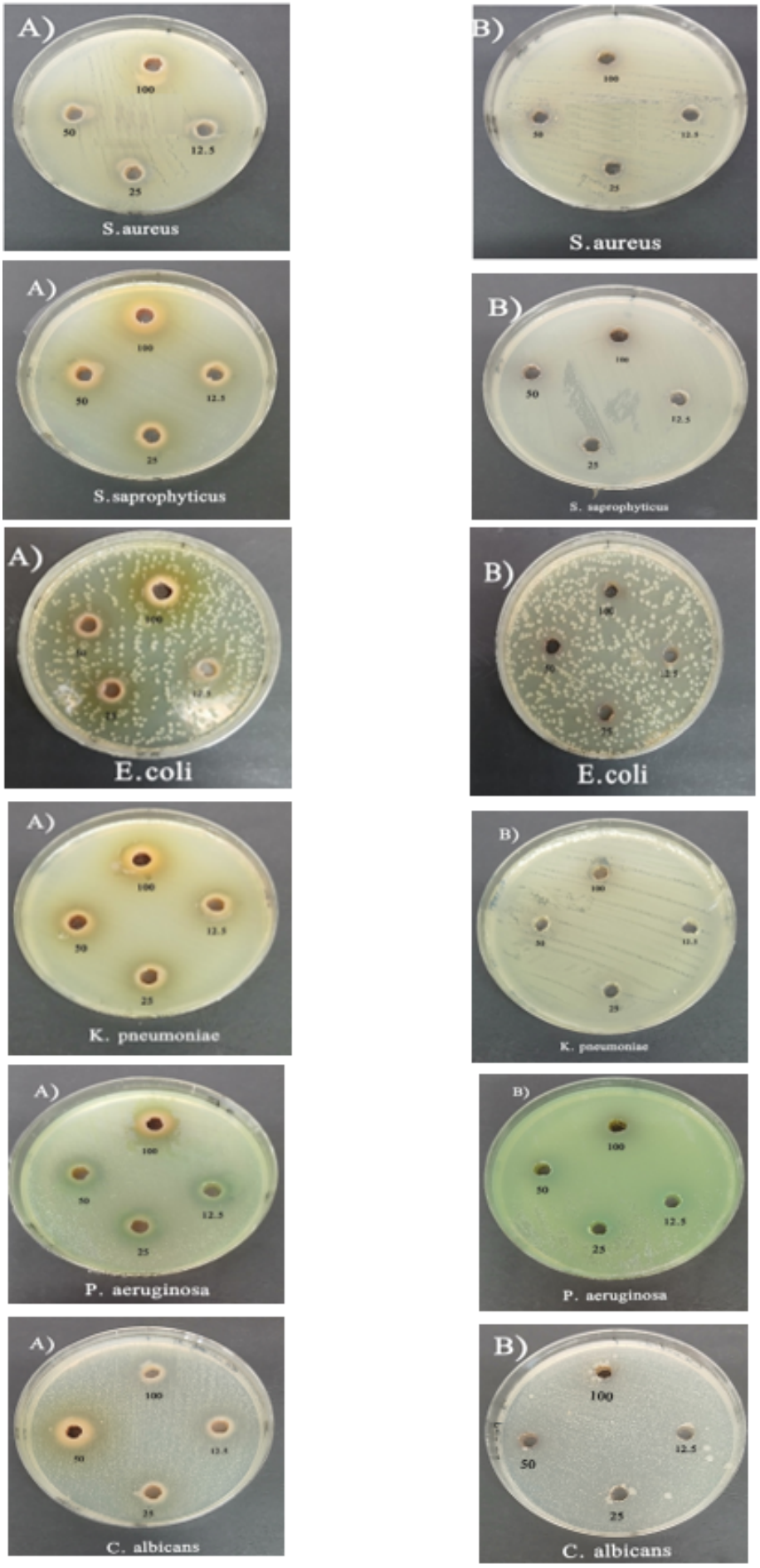

Figure 7. Antimicrobial activity: (A) Methanol Extract. (B) Methanol Rn-AgNPs

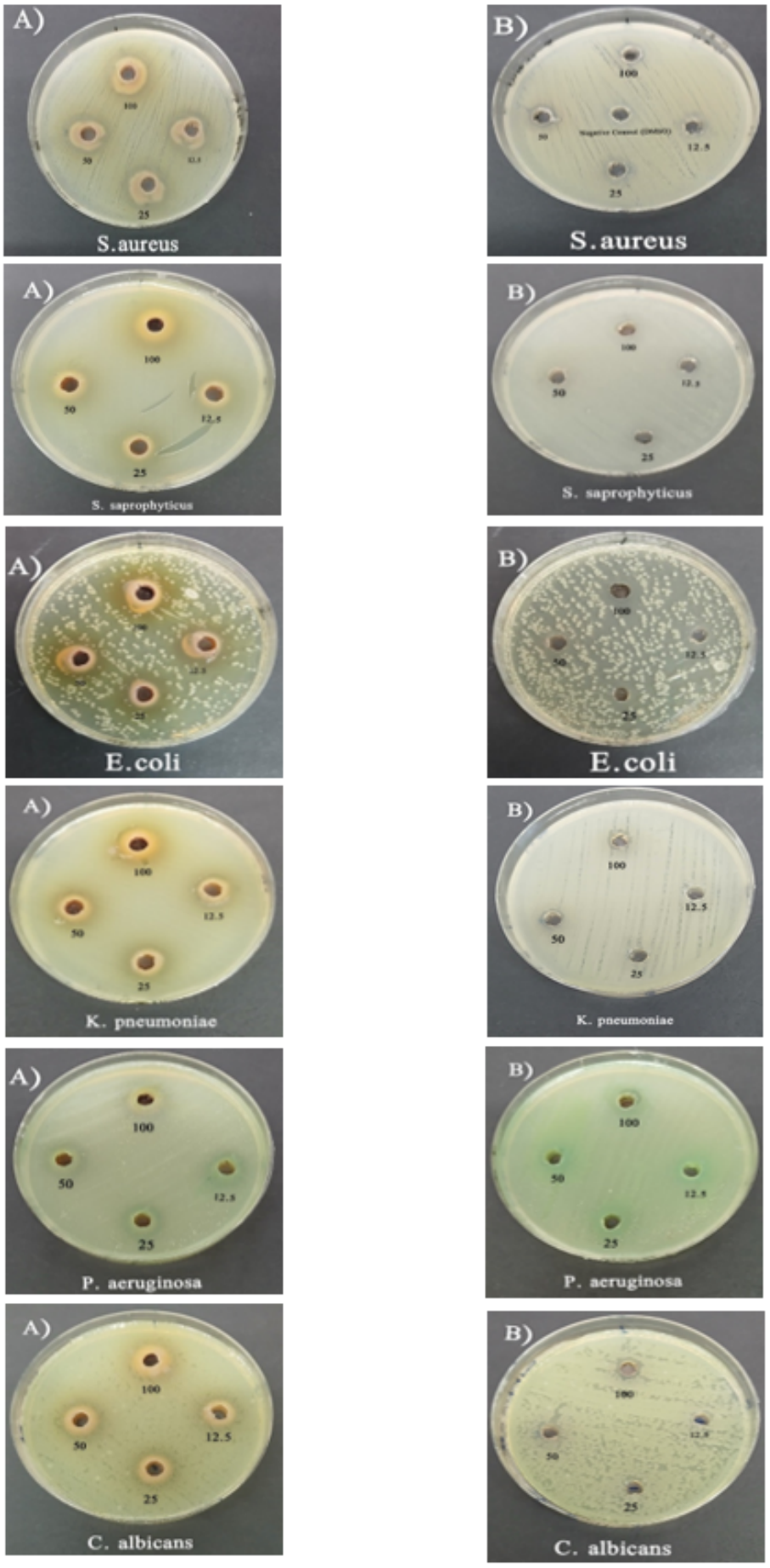

Figure 8. Antimicrobial activity: (A) Ethanol Extract. (B) Ethanol Rn-AgNPs

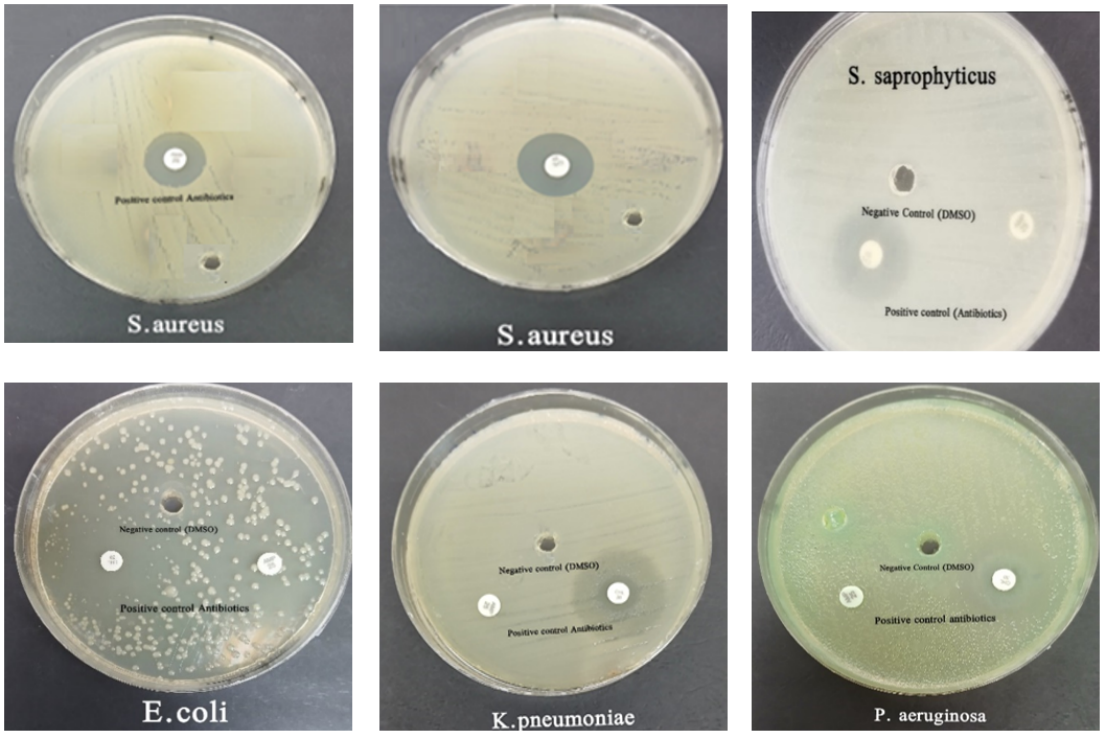

Figure 9. Negative control and anti-bacterial activity of antibiotics against the selected gram-positive and gram-negative bacteria

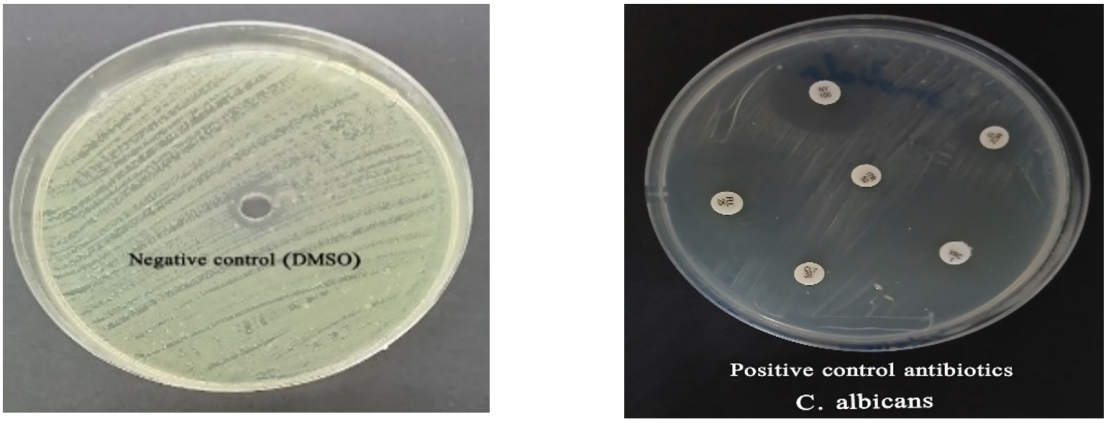

Figure 10. Negative control and anti-fungal activity of antibiotics against *C. albicans*

primarily focused on the leaves, our investigation reveals that floral and fruit extracts contain a unique concentration of polyphenols and flavonoids. This specific phytochemical profile results in nanoparticles with moderate to high colloidal stability and enhanced biological potency, as demonstrated by the calculated antioxidant activity and antimicrobial efficacy. Structural and spectroscopic analyses confirmed the efficient metal reduction and stabilization driven by these endogenous phytochemicals. The marked antioxidant efficiency of AgNPs and the selective yet potent antibacterial properties of the ethanolic formulations, quantitatively confirmed by their inhibitory concentrations and moderate to high negative zeta potential, support their potential integration into advanced antimicrobial and nanotherapeutic systems. The superior stability observed in the ethanolic-mediated AgNPs correlated with the higher antibacterial efficacy observed in this study, likely due to a more robust and bioactive capping layer. Future investigations should address cytotoxicity, release dynamics, and formulation engineering to further advance these biomedical and pharmaceutical applications.

5. RECOMMENDATION

Based on the current findings, we recommend employing High-Resolution Electron Microscopy (SEM/TEM) in future studies to provide more detailed morphological mapping and size distribution analysis. Furthermore, conducting comprehensive cytotoxicity assays against human cell lines is essential to evaluate the biocompatibility and safety of these biosynthesized AgNPs, which is a crucial step before their potential implementation in

medical and pharmaceutical applications.

REFERENCES

[1] A. B. Vimalanathan, V. Tyagi, A. Rajesh, P. Devanand, and M. G. Tyagi, "Biosynthesis of silver nanoparticles using chinese white ginseng plant root panax ginseng," *World J. Pharm. Pharm. Sci.*, vol. 2, no. 5, pp. 3632–3642, Oct. 2013.

[2] P. Kouvaris, A. Delimitis, V. Zaspalis, D. Papadopoulos, S. A. Tsipas, and N. Michailidis, "Green synthesis and characterization of silver nanoparticles produced using arbutus unedo leaf extract," *Mater. Lett.*, vol. 76, pp. 18–20, 2012. DOI: 10.1016/j.matlet.2012.02.025.

[3] S. S. Shankar, A. Rai, A. Ahmad, and M. Sastry, "Rapid synthesis of au, ag, and bimetallic au core–ag shell nanoparticles using neem (azadirachta indica) leaf broth," *J. Colloid Interface Sci.*, vol. 275, no. 2, pp. 496–502, 2004. DOI: 10.1016/j.jcis.2004.03.003.

[4] V. Kumar and S. K. Yadav, "Plant-mediated synthesis of silver and gold nanoparticles and their applications," *J. Chem. Technol. & Biotechnol.*, vol. 84, no. 2, pp. 151–157, 2009. DOI: 10.1002/jctb.2023.

[5] A. Dhaka, S. C. Mali, S. Sharma, and R. Trivedi, "A review on biological synthesis of silver nanoparticles and their potential applications," *Results Chem.*, vol. 6, p. 101 108, 2023. DOI: 10.1016/j.rechem.2023.101108.

[6] M. A. Ansari, H. M. Khan, A. A. Khan, S. S. Cameotra, and M. A. Alzohairy, "Anti-biofilm efficacy of silver nanoparticles against mrsa and mrse isolated from wounds in a tertiary care hospital," *Indian J. Med. Microbiol.*, vol. 33, no. 1, pp. 101–109, 2015. DOI: 10.4103/0255-0857.148402.

[7] K. T. Desta et al., "Dietary-flavonoid-rich flowers of rumex nervosus vahl: Lc-ms profiling and anti-inflammatory effects," *J. Sep. Sci.*, vol. 38, no. 19, pp. 3345–3353, 2015. DOI: 10.1002/jssc.201500737.

[8] A. H. M. M. Rahman, M. Anisuzzaman, S. A. Haider, F. Ahmed, A. K. M. R. Islam, and A. T. M. Naderuzzaman, "Study of medicinal plants in the graveyards of rajshahi city," *Res. J. Agric. Biol. Sci.*, vol. 4, no. 1, pp. 70–74, 2008.

[9] A. Getie, T. Mariam, R. Reitz, and R. H. Neubert, "Evaluation of antimicrobial and anti-inflammatory activities of medicinal plants," *Fitoterapia*, vol. 74, no. 1–2, pp. 139–143, 2003. DOI: 10.1016/s0367-326x(02)00315-5.

[10] M. M. Quradha, R. Khan, M. Rehman, and A. Abohajeb, "Chemical composition and in vitro anticancer, antimicrobial and antioxidant activities of essential oil and methanol extract from rumex nervosus," *Nat. Prod. Res.*, vol. 33, no. 17, pp. 2554–2559, 2019. DOI: 10.1080/14786419.2018.1452009.

[11] M. Al-Nowihi, A. Faisal, and G. Al-Asbahi, "Antimicrobial activity of rumex nervosus extract collected from yemen against local selected isolates pathogens," *J. Microbiol. & Exp.*, vol. 8, no. 3, pp. 93–96, 2020.

[12] A. W. Alshameri et al., "Rumex nervosus mediated green synthesis of silver nanoparticles and evaluation of antibacterial and cytotoxic activity," *OpenNano*, vol. 8, p. 100 084, 2022. DOI: 10.1016/j.onan.2022.100084.

[13] A. Chakravarty et al., "Green synthesis of silver nanoparticles using syzygium cumini fruit extracts," *Chem. Phys. Lett.*, vol. 795, p. 139 493, 2022. DOI: 10.1016/j.cplett.2022.139493.

[14] J. B. Harborne, *Phytochemical Methods: A Guide to Modern Techniques of Plant Analysis*, 3rd ed. London, UK: Chapman & Hall, 1998.

[15] E. M. Elsebaie et al., "Silver nanoparticle synthesis by rumex vesicarius extract and its applicability against foodborne pathogens," *Foods*, vol. 12, no. 9, p. 1746, 2023.

[16] A. A. H. Abdellatif, M. A. H. Mostafa, H. Konno, and M. A. Younis, "Exploring the green synthesis of silver nanoparticles using natural extracts and their potential for cancer treatment," *3 Biotech*, vol. 14, no. 11, p. 274, 2024. DOI: 10.1007/s13205-024-04118-z.

[17] A. M. Awwad and N. M. Salem, "Green synthesis of silver nanoparticles by mulberry leaves extract," *Nanosci. Nanotechnol.*, vol. 2, no. 4, pp. 125–128, 2012. DOI: 10.5923/j.nn.20120204.06.

[18] S. Ahmed, M. Ahmad, B. L. Swami, and S. Ikram, "A review on plant extract mediated synthesis of silver nanoparticles for antimicrobial applications: A green expertise," *J. Adv. Res.*, vol. 7, no. 1, pp. 17–28, 2016. DOI: 10.1016/j.jare.2015.02.007.

[19] A. D. Fraia et al., "Green synthesis of silver nanoparticles (ag-nps) from g. stearothermophilus gf16: Stable and versatile nanomaterials with antioxidant, antimicrobial, and catalytic properties," *Microb. Cell Factories*, vol. 24, no. 1, p. 189, 2025. DOI: 10.1186/s12934-025-02512-x.

[20] H. M. Ibrahim, A. A. Humaid, A. A. M. Thabit, E. A. Rizq, and B. H. Al-awadhi, "Phytochemical screening, antioxidant and antimicrobial activities of acacia origena hunde," *J. Chem. Biol. Phys. Sci. B*, vol. 13, no. 3, pp. 308–321, 2023. DOI: 10.24214/jcbps.B.13.3.30821.

[21] G. Al-Naqeb, "Antioxidant and antibacterial activities of some yemeni medicinal plants," *Int. J. Herb. Med.*, vol. 3, no. 1, pp. 6–11, 2015.

[22] J. Sebaugh, "Guidelines for accurate ec50/ic50 estimation," *Pharm. Stat.*, vol. 10, no. 2, pp. 128–134, 2011. DOI: 10.1002/pst.426.

[23] Y. Chen et al., "Optimizing drug sensitivity assays in patient-derived tumor organoids: A comparison of ic50 estimation methods and experimental parameters," *Biol. Methods Protoc.*, vol. 10, no. 1, bpaf012, 2025. DOI: 10.1093/biomethods/bpaf012.

[24] H. M. Ibrahim, Q. Y. M. Abdullah, A. A. Humaid, A. A. M. Thabit, S. M. Al-Alawi, and A. T. Al-Ramsi, "Phytochemical screening and anti-microbial activities of aloe fleurentinorum lavranos newton," *J. Chem. Biol. Phys. Sci. B*, vol. 12, no. 3, pp. 335–348, 2022. DOI: 10.24214/jcbps.B.12.3.33548.

[25] M. Hiregoudar et al., "Antibacterial activity of some spice extracts on streptococcus mutans: An in vitro study," *J. Indian Assoc. Public Health Dent.*, vol. 9, no. 1, S347–S351, 2011.

[26] B. M. Al-Attab, M. A. Almaqtari, and A. Y. Mubarak, "Antioxidant and antimicrobial of three extracts of caralluma deflersiana laver," *Sana'a Univ. J. Appl. Sci. Technol.*, vol. 2, no. 2, pp. 154–157, 2024. DOI: 10.59628/jast.v2i2.862.

[27] N. Baeshen et al., "Gc-ms analysis of bioactive compounds extracted from plant rhazya stricta using various solvents," *Plants*, vol. 12, no. 4, p. 960, 2023. DOI: 10.3390/plants12040960.

[28] I. Batubara et al., "Phytochemical profile and in vitro–in silico antibacterial activity of melia azedarach leaf and twig extracts obtained using solvents of different polarities," *Science*, vol. 7, no. 4, p. 167, 2025. DOI: 10.3390/sci7040167.

[29] K. T. Desta et al., "Dietary-flavonoid-rich flowers of rumex nervosus vahl: Lc-ms profiling and anti-inflammatory effects," *J. Sep. Sci.*, vol. 38, no. 19, pp. 3345–3353, 2015. DOI: 10.1002/jssc.201500737.

[30] V. Sharma, D. Verma, and G. S. Okram, "Influence of surfactant, particle size and dispersion medium on surface plasmon resonance of silver nanoparticles," *J. Physics: Condens. Matter*, vol. 32, no. 14, p. 145 302, 2020. DOI: 10.48550/arXiv.1908.03064.

[31] K. Okaiyeto, M. O. Ojemaye, H. Hoppe, L. V. Mabinya, and A. I. Okoh, "Green synthesis of silver nanoparticles using microbial extracts," *Molecules*, vol. 24, no. 23, p. 4382, 2019. DOI: 10.3390/molecules24234382.

[32] P. B. E. Kedi et al., "Biosynthesis of silver nanoparticles from microsorum punctatum fronds extract and in-vitro anti-inflammation study," *J. Nanotechnol. Res.*, vol. 2, no. 2, pp. 25–41, 2020. DOI: 10.26502/jnr.2688-85210014.

[33] A. Ansari, S. Sachar, and S. S. Garje, "Synthesis of tio2 nanoparticles and their interactions with serum albumin," *New J. Chem.*, vol. 42, no. 16, pp. 13 511–13 523, 2018. DOI: 10.1039/C8NJ02253D.

[34] I. Fernando and Y. Zhou, "Impact of ph on stability, dissolution and aggregation kinetics of silver nanoparticles," *Chemosphere*, vol. 216, pp. 297–305, 2019. DOI: 10.1016/j.chemosphere.2018.10.122.

[35] Z. Iskakova et al., "Green synthesis of silver nanoparticles using circaea lutetiana ethanolic extract: Phytochemical profiling and antimicrobial evaluation," *Int. J. Mol. Sci.*, vol. 26, no. 12, p. 5505, 2025. DOI: 10.3390/ijms26125505.

[36] S. Alzarea et al., "Nutraceutical rumex nervosus as a natural drug candidate: Metabolite profiling and pharmacological estimation," *Molecules*, vol. 29, no. 14, p. 3315, 2024. DOI: 10.2174/0113816128360594250725110421.

[37] Z. Bedlovičová, I. Strapáč, M. Baláž, and A. Salayová, "Overview on antioxidant activity determination of silver nanoparticles," *Molecules*, vol. 25, no. 14, p. 3191, 2020. DOI: 10.3390/molecules25143191.

[38] K. Younes et al., "In-vitro antioxidant and antiradical potential of rumex vesicarius and its silver nanoparticles," *Notulae Bot. Horti Agrobot. Cluj-Napoca*, vol. 49, no. 1, p. 12 293, 2021. DOI: 10.15835/nbha49112293.

[39] M. Motene, C. Maepa, and M. Sigidi, "Optimizing antimicrobial, antioxidant and cytotoxic properties of silver nanoparticles synthesized from elephantorrhiza elephantina," *Plants*, vol. 14, no. 5, p. 822, 2025. DOI: 10.3390/plants14050822.

[40] M. Qureshi, F. Ghori, M. Idrees, Z. Zafar, F. Naseer, and M. Ahmed, "Comparative analysis of fagonia indica extracts and green synthesized nanoparticles for antioxidant potential," *Sci. Reports*, vol. 15, p. 20 232, 2025. DOI: 10.1038/s41598-025-20232-1.

[41] M. Stančiauskaitė, M. Marksa, L. Babickaitė, D. Majiene, and K. Ramanauskienė, "Comparison of ethanolic and aqueous populus balsamifera extracts: Composition and biological activities," *Pharmaceuticals*, vol. 14, no. 10, p. 1018, 2021. DOI: 10.3390/ph14101018.

[42] P. Altavas et al., "Antimicrobial activity of ardisia serrata ethanolic and aqueous leaf extract," *Acta Medica Philipp.*, vol. 58, pp. 91–97, 2024. DOI: 10.47895/amp.vi0.6160.

[43] Y. El-Sawy, A. Abdel-Salam, H. Abd-Elhady, K. Abou-Taleb, and R. Ahmed, "Elimination of listeria monocytogenes biofilms using natural plant extracts," *Sci. Reports*, vol. 14, 2024. DOI: 10.1038/s41598-024-52394-9.

[44] D. L. Scaramussa, L. D. A. Soares, and L. Santana, "Antioxidant and antimicrobial activities of hymenaea courbaril extracts," *Food Sci. Technol. Int.*, vol. 30, pp. 128–136, 2022. DOI: 10.1177/10820132221136589.

[45] P. Arya, D. Vaidya, M. Kaushal, S. Devi, A. Gupta, and S. Chand, "Effect of solvents on phytochemical constituents and antimicrobial activity of boehmeria rugulosa," *Sci. Reports*, vol. 15, 2025. DOI: 10.1038/s41598-025-14506-x.

[46] S. Al-Arnoot et al., "Multitarget antimicrobial mechanisms of plant extracts: A review of harnessing phytochemicals against drug-resistant pathogens," *Sana'a Univ. J. Med. Health Sci.*, vol. 19, no. 4, pp. 292–309, 2025.

[47] A. Gaurav, P. Bakht, M. Saini, S. Pandey, and R. Pathania, "Role of bacterial efflux pumps in antibiotic resistance, virulence, and strategies to discover novel efflux pump inhibitors," *Microbiology*, vol. 169, 2023.

[48] F. A. Alhadi, S. T. Atta, and H. M. Ibrahim, "Phytochemical screening and selected biological activities of solanum incanum l. fruit extracts," *PSM Microbiol.*, vol. 10, no. 1, pp. 122–136, 2025.

[49] A. B. Lorusso, J. A. Carrara, C. D. Barroso, F. F. Tuon, and H. Faoro, "Role of efflux pumps on antimicrobial resistance in pseudomonas aeruginosa," *Int. J. Mol. Sci.*, vol. 23, 2022.

[50] M. Nabi et al., "Phytochemical profiling and antibacterial activity of methanol leaf extract of skimmia anquetilia," *Plants*, vol. 11, 2022. DOI: 10.3390/plants11131667.

[51] O. Contreras-Martínez, D. Sierra-Quiroz, and A. Angulo-Ortíz, "Antibacterial and antibiofilm potential of ethanolic extracts of duguetia vallicola against pseudomonas aeruginosa," *Plants*, vol. 13, 2024. DOI: 10.3390/plants13101412.

[52] V. Dhanapal et al., "Green synthesis of silver nanoparticles using woodfordia flower extracts for bacterial inhibition applications," *Heliyon*, vol. 11, 2025. DOI: 10.1016/j.heliyon.2025.e42125.

[53] M. Motene, C. Maepa, and M. Sigidi, "Optimizing antimicrobial, antioxidant, and cytotoxic properties of silver nanoparticles synthesized from elephantorrhiza elephantina extracts," *Plants*, vol. 14, 2025. DOI: 10.3390/plants14050822.

[54] M. Devi, S. Devi, V. Sharma, N. Rana, R. Bhatia, and A. Bhatt, "Green synthesis of silver nanoparticles using aegle marmelos fruit extract and antimicrobial potential," *J. Tradit. Complementary Med.*, vol. 10, pp. 158–165, 2019. DOI: 10.1016/j.jtcme.2019.04.007.